

Analytical Methods

Accepted Manuscript



This is an *Accepted Manuscript*, which has been through the Royal Society of Chemistry peer review process and has been accepted for publication.

Accepted Manuscripts are published online shortly after acceptance, before technical editing, formatting and proof reading. Using this free service, authors can make their results available to the community, in citable form, before we publish the edited article. We will replace this *Accepted Manuscript* with the edited and formatted *Advance Article* as soon as it is available.

You can find more information about *Accepted Manuscripts* in the [Information for Authors](#).

Please note that technical editing may introduce minor changes to the text and/or graphics, which may alter content. The journal's standard [Terms & Conditions](#) and the [Ethical guidelines](#) still apply. In no event shall the Royal Society of Chemistry be held responsible for any errors or omissions in this *Accepted Manuscript* or any consequences arising from the use of any information it contains.

1 **The fast and direct characterization of blue-and-white porcelain**
2 **glaze from Jingdezhen by laser ablation-inductively coupled**
3 **plasma mass spectrometry**

4
5 Zhian BAO^{*}, Honglin YUAN^{*†}, Rui WEN^{**}, Kaiyun CHEN^{*}

6 ^{*} *State Key Laboratory of Continental Dynamics, Department of Geology,*
7 *Northwest University, Xi'an 710069, China*

8 ^{**} *School of Culture Heritage, Northwest University, Xi'an 710069, China*

9
10
11
12
13
14
15
16
17
18
19
20
21
22
23
24
25
26
27
28
29
30
31
32
33
34
35
36
37
38
39
40
41
42
43
44
45
46
47
48
49
50
51
52
53
54
55
56
57
58
59
60

[†] Corresponding author: Yuan Honglin, email: yhlsklcd@126.com

1
2
3
4
5
6
7
8
9
10
11
12
13
14
15
16
17
18
19
20
21
22
23
24
25
26
27
28
29
30
31
32
33
34
35
36
37
38
39
40
41
42
43
44
45
46
47
48
49
50
51
52
53
54
55
56
57
58
59
60

19 **Abstract:** This study evaluated the classification of blue-and-white porcelains of
20 Jingdezhen during the Ming Dynasties based on elemental concentrations measured by
21 laser ablation-inductively coupled plasma mass spectrometry (LA-ICP-MS). The
22 blue-and-white porcelains of the Ming Dynasties are subdivided into three periods:
23 Hongwu (HW), Xuande (XD) and Wanli (WL), representing to early Ming, middle Ming
24 and late Ming Dynasties, according to Fe-Mn-Co distribution and Co contents. We propose
25 ratios of Fe/Mn ratio and Co contents in light-blue areas as criterion to identify the
26 classification of blue-and-white porcelains of Jingdezhen. The reference value of Fe/Mn of
27 HW, XD and WL are 11.9 ± 0.39 , 2.31 ± 0.54 , and 7.09 ± 2.07 $\mu\text{g/g}$, while the cobalt
28 concentration of HW, XD and WL porcelains are <100 $\mu\text{g/g}$, $500\text{-}600$ $\mu\text{g/g}$ and >2500 $\mu\text{g/g}$,
29 respectively. Other elements, including Li, B, Mn, Ni, Cr, Ho, Pb, Th, U and rare earth
30 elements can also assist identification of the blue-and-white porcelain classification. Further
31 measurements of more blue-and-white porcelains need to be analyzed using LA-ICP-MS to
32 get more elemental concentration and obtain statistical database for blue-and-white
33 porcelain identification.

36 **Keywords:** LA-ICP-MS; blue-and-white porcelain; Fe/Mn; Cobalt pigment; trace elements

38

39 Introduction

40 Blue-and-white porcelain was underglaze faience, which was painted on the body
41 using cobalt pigment and presented dark blue, light blue and white after single firing. The
42 Yuan (AD 1271-1368) and Ming (AD 1368-1644) Dynasties witnessed the development of
43 the technique of blue-and-white porcelain: during the 80 years from the 1320s to the early
44 15th century, the blue-and-white porcelain made in Jingdezhen soon became the
45 mainstream of Chinese porcelain production¹. The Jingdezhen official kiln, also named the
46 Guan kiln, was managed by the government. The production of the Jingdezhen Guan kiln
47 represented the highest quality amongst the contemporaneous porcelain. The source of the
48 pigment ore, the selection procedure and the machining process were subject to strict
49 criteria and regulations, so the chemical composition of porcelain made in the Jingdezhen
50 Guan kiln was uniform within one period and shows variations between different periods².
51 Cobalt pigment was imported from other countries to China in the Yuan and early Ming
52 Dynasties³⁻⁵, while domestic asbolane began to be used in the early Ming Dynasty. A mixed
53 pigment composed by both imported and domestic origin was used in late Ming Dynasty.

54 The differences in cobalt ore sources, glaze components and manufacture techniques
55 result in elemental concentration variations of porcelain, which provide the basis for
56 authenticating the ancient ceramic origin, chronology, circulation and truth. Several
57 analytical techniques has been applied in the major and trace elemental analysis of ceramics,
58 including neutron activation analysis (NAA), energy dispersive X ray fluorescence
59 (EDXRF), scanning electron microscopy (SEM), electron microprobe analysis (EMPA),
60 time of flight mass spectrometer (TOF), thermal ionization mass spectrometer (TIMS),
61 laser induced breakdown spectroscopy (LIBS), laser ablation/solution nebulization
62 inductively coupled plasma mass spectrometry (LA/SN-ICP-MS), and SN-inductively
63 coupled plasma atomic emission spectrometry (SN-ICP-AES)^{3, 6-16}. SN-ICP-MS, TIMS,
64 SN-ICP-AES and NAA techniques are rarely used in archaeological research due to
65 chemical digestion of 50 mg to 5g sample powder during sample preparation prior to
66 instrumental analyses. Although EDXRF and EMPA are an undamaged-analysis technique,

1
2
3
4
5
6
7
8
9
10
11
12
13
14
15
16
17
18
19
20
21
22
23
24
25
26
27
28
29
30
31
32
33
34
35
36
37
38
39
40
41
42
43
44
45
46
47
48
49
50
51
52
53
54
55
56
57
58
59
60

67 its high detection limits lead to the non-accurate trace element measurement. The
68 LA-ICP-MS is an in-situ micro analytical technique for accurate multiple-elemental
69 contents measurements with low detection limit and high spatial resolution, and can be
70 applied in archeologist research based on trace element concentration analyses.

71 In this work, we used the LA-ICP-MS technique to analyze trace elemental
72 concentrations of ancient Chinese blue-and-white porcelains from Guan kiln of the Yuan
73 dynasty, the Ming dynasty and the Qing dynasty in Jingdezhen, Jiangxi province for the
74 first time. The Ming Dynasty can be further divided into three periods, early Ming, middle
75 Ming and late Ming Dynaties. The three subdivision of Ming dynasty were also named
76 Hongwu (HW, Hongwu-Yongle, AD 1368-1424), Xuande (XD, Xuande-Hongzhi, AD
77 1426-1505) and Wangli (WL, Zhengde-Wanli, AD 1506-1620) periods, respectively. Three
78 typical blue-and-white porcelains fragments (Fig 1) were manufactured in Hongwu,
79 Xuande and Wangli periods, which were excavated from Jingdezhen Guan kiln site in 2002.
80 They were selected to investigate the possibilities to clarify the blue-and-white porcelains
81 based on trace elemental concentrations and ratios measured by LA-ICP-MS.

82 83 **Methods and techniques**

84 **Instruments**

85 In this work, micro in situ analysis of ceramic fragments was carried out by using laser
86 ablation (GeoLas LA, Coherent, USA) coupled with a Quadrupole ICP-MS (Agilent 7700a
87 ICP-MS, USA). In the LA system, the 193nm UV laser beam coming from the Compex102
88 laser unit (Lambda Physik, Germany) underwent homogenization, enabling flat-topped
89 laser beam. The diameter of laser ablated spot sizes are varied from 5 to 120 μm with the
90 homogeneous energy density distribution¹⁷. A home-made homogenizer is applied between
91 the sample cell and ICP torch to obtain smooth signal. High purity helium gas (99.9995%)
92 was used as the carrier gas. All LA-ICP-MS measurements were carried out using time
93 resolved analysis (TRA) mode, which operated in a fast, peak jumping mode. Signal
94 intensities were around 2M cps for 60 μm spot size in terms of uranium in NIST (National
95 Institute of Standards and Technology, USA) Standard Reference Material 610. Each spot

1
2
3 96 analyses consisted of approximately 25s background, 3s of pre-ablation, and followed with
4
5 97 40s data acquisition. The pre-ablation step can remove any contamination on the sample
6
7 98 surface. The ICP-MS instrument settings were optimized aiming at maximum and stable
8
9 99 signal intensities, low oxide ratio and low double charge ratio for all analytes. Detailed
10
11 100 instrumental parameters are summarized in Table 1. A scanning electron microscope (SEM,
12
13 101 FEI Quanta FEG) was used for evaluating the laser ablated craters and the thickness of
14
15
16 102 glaze.

17
18 103

104 **Procedure for the characterization of different areas by LA-ICP-MS**

105 Prior to analyses, the surface of the porcelain fragments was cleaned with high pure
106 water ($18.2\text{M}\Omega\cdot\text{cm}^{-1}$, MilliQ-E) for about 5 min in ultrasonic bath. In order to obtain
107 representative values for every ceramic fragment, several sampling positions were analyzed
108 including dark-blue area (Co-enriched), light-blue area (Co-medial) and white glaze area
109 (Co-least). Each ablation consisted of 200 laser pulses. At each spot, the sample surface was
110 ablated for 3s to remove any contamination prior to real analyses. The signal of $^{59}\text{Co}^+$ was
111 monitored to prevent from ablating the ceramic bodies (Fig 2), and the craters were
112 examined finally by SEM with the acceleration voltage 20 kv, and the current 0.6 nA. NIST
113 610 was used for external calibration, while SiO_2 obtained by EDXRF was used as internal
114 standard (IS). The LA-ICP-MS data was reduced by ICPMSDataCal software¹⁸.

115

116 **Results and Discussion**

117 **Characterization of laser ablated craters of porcelain**

118 Fig 3 shows the section of porcelain and spot quality of laser ablated crater. The
119 porcelain can be divided into two layers, the glaze layer and the body. The glazer layer is
120 about 400 μm in thickness, while the top 280 μm part is free of hole (Fig 3A). The depth of
121 the laser ablated crater is about 30 μm (Fig 3B) which can guarantee the crater is inside the
122 hole-free glaze layer. The laser ablated carter shows round, deep and flat bottom characters,
123 which reveals that the excimer laser can ablate the blue-and-white porcelain effectively (Fig
124 3B). Each crater consumed less than 1 μg sample with 60 μm spot sizes in diameter, which

1
2
3 125 is hardly observed with naked eye.
4
5
6

7
8
9
10
11
12
13
14
15
16
17
18
19
20
21
22
23
24
25
26
27
28
29
30
31
32
33
34
35
36
37
38
39
40
41
42
43
44
45
46
47
48
49
50
51
52
53
54
55
56
57
58
59
60

126
127 **Comparison of Fe/Mn ratios and Co concentration in different areas of the**
128 **blue-and-white porcelain**

129 Fe/Mn ratio of light-blue areas of porcelain changed systematically of different periods
130 and could be served as a criterion to identify the period of the blue-and-white porcelain
131 since the blue area of the porcelain represents the original pigment, which can be used to
132 trace the ore sources and the ore source is not changed during the same period^{6, 13, 19}. The
133 Mn, Fe and Co concentrations of white, light-blue and dark-blue areas of the three selected
134 samples of HW, XD and WL periods measured in this work are listed in Table 2. The Mn
135 concentration of both light-blue and dark-blue areas of HW is relatively lower than that of
136 both XD and WL. The Mn contents of all blue areas of XD are higher than that of XL. The
137 dark-blue and light-blue areas of XD porcelains show 20x and 5x higher Mn contents than
138 that of HW porcelains, and 5.9x and 1.6x higher than that of WL porcelains. The Fe
139 contents show different distribution among these blue-and-white porcelains comparing to
140 Mn concentration. The Fe concentration of both white and light-blue areas of the
141 blue-and-white porcelains of WL is almost 2x higher than others measured in this work
142 which may indicate that the modification during late Ming Dynasty. The average Fe/Mn
143 ratios of white areas of porcelains of HW and XD are close to 11 (10.8-11.4), which is
144 lower than that of porcelains of WL ($\text{Mean}_{\text{Fe/Mn}}=14.9\pm 0.3$). It is fairly difficult to
145 distinguish the differences between different period of porcelain with only Fe/Mn ratios in
146 white glaze areas. However, the Fe/Mn ratios in light-blue areas of HW, XD, WL, are
147 11.9 ± 0.39 , 2.31 ± 0.54 , and 7.09 ± 2.07 $\mu\text{g/g}$, which is the same as Wen's conclusion¹³ that
148 the Fe/Mn values exceed 11 in the early Ming period, lower than 2.5 in the middle Ming
149 period and 3~10 in the late Ming period.

150 Co is a candidate tracer besides Mn and Fe due to significant variations light-blue and
151 white areas of porcelains of different periods. The light-blue areas of porcelains of HW, XD
152 and WL periods have different Co concentration ranging from <100, 500-600 and >2500
153 ppm. The Co contents of white areas of the HW, XD and WL porcelains are <2, ~10,

1
2
3 154 and >20 $\mu\text{g/g}$ which are much lower than that of both light-blue and dark-blue area of the
4
5 155 blue-and-white porcelains of the three periods. The Co contents of light-blue area of
6
7 156 porcelain of the three Dynasties are >40X of that of white areas of porcelains of the same
8
9 157 sample, while the dark-blue areas show 100X higher than that of the white areas. The
10
11 158 phenomenon could be caused by dark spots, which are the result of crystallization and
12
13 159 enrichment of manganese and iron contained in cobalt blue pigment after high-temperature
14
15 160 sintering.²⁰

161 Analysis of the iron, manganese and cobalt correlation in light-blue areas allows us to
162 identify the blue-and-white porcelains of the Ming Dynasties. In Figure 4 the triangular
163 correlation plot of Fe, Mn and Co is displayed. These three elements in light-blue areas
164 seem to have the ability to group the porcelains in three different clusters, while these
165 elements in white areas are difficult to identify the porcelains, as can be visualized in the
166 ternary plot.

167

168 Trace elements in dark-Blue areas

169 One of the advantages of the LA-ICP-MS technique is that it can measure trace
170 element concentrations with great accuracy and precision, as well as low detection limit
171 (down to ppb level for most elements). The elemental concentration of the dark-blue areas
172 of the blue-and-white porcelains of HW, XD and WL are more heterogeneous than that of
173 light-blue and white areas due to some dark spots which concentrated in Co, Fe and REEs.
174 The elemental concentration of the dark-blue areas of blue-and-white porcelains could be
175 used to justify the source of the ore since these areas are more concentrated of pigments.
176 Most elements (including Be, B, P, Mn, Fe, Ni, Cu, Zn, Ge, Sn, Ce, Ta, W, Pb, U and T_{REE}
177 (total rare earth elements)) of dark-blue areas of porcelains of WL samples show middle
178 concentration between the HW and XD, which indicates that the pigments of WL are the
179 mixture of those used for HW and XD and this agrees with earlier results^{13, 19} that the
180 pigments of HW is imported while that of XD was local, and both imported and local
181 pigments are mixed in WL period(Fig 5). All porcelain samples show similar chondrite
182 normalized REE distribution (Fig 6) while the HW shows low REE contents and XD

183 samples show higher REE concentrations with positive Ce anomalies. The REEs
184 concentrations of WL samples are between relative HW and XD samples which illustrate
185 that the pigments applied in WL period are the mixture of imported pigments at HW period
186 and local pigments at XD period.

187

188 **The possible ore source used as the cobalt pigment in different periods**

189 Some elements are taken into account to evaluate the possible ore source, including Fe,
190 Mn and Co, as well as other elements which could be associated to cobalt, like Cu, Pb, As
191 and Ni. Cu is characteristic of the HW samples for its high correlation coefficient
192 ($R^2=0.9353$), but it seems to be poor correlated (R^2 value are 0.2862) in the XD samples but
193 intermediate in WL samples ($R^2=0.6004$). Similarly, As becomes distinctive in the Hw
194 samples for its high correlation ($R^2=0.8797$), while it is poor correlated ($R^2 =0.0007$) in XD
195 samples and intermediate correlated ($R^2=0.6532$) in WL samples. Fe also has the similar
196 behavior as Cu and As (R^2 values are 0.9926 in HW samples, 0.7638 in WL samples, and
197 0.3622 in XD samples). Pb is an element with high correlation with Co in the three samples
198 (R^2 values are 0.6908 in HW, 0.8251 in XD and 0.3491 in WL). In XD samples, Mn have
199 the highest correlation proportion ($R^2=0.9715$) apart from Ni ($R^2=0.5255$) and Li
200 ($R^2=0.4052$). Based on the elemental correlations, cobalt pigments of each sample could be
201 summarized as: Co-Fe-Cu-Zn-Pb (As) for HW samples, Co-Mn-Pb-Ni-Zn-Li for XD
202 samples and Co-Fe-As-Cu-Pb for WL samples (elements in parentheses correlate to Co but
203 low in the pigment; Fig.7 show the values of Mn, Pb, and Ni correlation coefficient with Co
204 in XD samples).

205 Due to the high concentration and high correlation coefficient of Fe, Cu and Zn with
206 Co in HW samples and cobalt production is usually linked to chalcopyrite (CuFeS_2) or
207 pyrite (FeS_2), even sphalerite ($\text{Zn,Fe} \text{S}$), cobalt source should be related to a
208 cobalt-associated copper mineral or iron mineral, which could have been a probable source
209 in the Yuan and early Ming periods. In the middle Ming dynasty, domestic asbolane
210 ($(\text{Co,Ni})\text{OMnO}_2 \cdot n\text{H}_2\text{O}$) is applied in the blue-and-white porcelain manufacture, which is
211 composed of lithiophorite ($(\text{Al,Li})\text{MnO}_2(\text{OH})_2$), vernadite ($\text{MnO}_2 \cdot n\text{H}_2\text{O}$) and ebelmenite.

1
2
3 212 The combination of the ores explains high correlation coefficient for Mn, Ni and Li in XD.
4
5 213 Some asbolane deposits were also exploited in Zhejiang, Jiangxi and Yunnan provinces,
6
7 214 and began to be widely used in Middle Ming¹³. The correlation coefficient of Fe, Cu and As
8
9 215 are intermediate between HW and XD samples, and the correlation coefficient of Li, Zn,
10
11 216 Mn are lowest in WL samples, which proves again that the mixture of imported pigments
12
13 217 and domestic asbolane were used in late Ming period.
14
15
16 218

17 219 **Conclusions**

19 220 Our study demonstrates that high-precise/accurate LA-ICP-MS trace element analysis
20
21 221 is very powerful for charactering of blue-and-white porcelain by the Fe-Mn-Co and REEs
22
23 222 concentration distributions of the pigment. The blue-and-white porcelains of Ming Dynasty
24
25 223 can be divided into three phases: HW, XD and WL, based on the ratios of Fe/Mn ratio and
26
27 224 cobalt concentrations in light-blue areas. The reference value of Fe/Mn of HW, XD and WL
28
29 225 in light-blue areas are 11.9 ± 0.39 , 2.31 ± 0.54 , and 7.09 ± 2.07 $\mu\text{g/g}$, respectively. The cobalt
30
31 226 concentration of light-blue area of HW porcelains are lower than 100 $\mu\text{g/g}$, which is
32
33 227 distinguished from that of XD porcelains (500-600 $\mu\text{g/g}$) and WL porcelains (>2500 $\mu\text{g/g}$).
34
35 228 The LA-ICP-MS may be a very promising method for archaeological materials research
36
37 229 due to its ability of measurement of more than 40 elements with low detection limit. Further
38
39 230 work need to be done to analysis more blue-and-white porcelains to obtain statistical
40
41 231 meaningful database for blue-and-white porcelain identification.
42
43
44 232

45 233 **Acknowledgements**

46
47 234 This work was co-supported by the National Natural Science Foundation of China (Grants
48
49 235 41373004) and the State Key Laboratory of Independent Research Key Topics of Special
50
51 236 Funds from the Ministry of Science and Technology (BJ08132-1, BJ14269). We are also
52
53 237 grateful to the anonymous reviewers for their constructive comments.
54
55 238

56 239 **Reference**

57
58
59 240 1. X. Feng, *Chiese ceramics*, shanghai Classic Publishing House, shanghai. 2001.
60

- 1
2
3 241 2. B. Geng, *Identification of porcelain of Ming and Qing Dynasties*, Zi-jin-cheng
4 Publishing House and Liang-mu Publishing House. 1993.
5
6 242
7 243 3. Y. Chen, F. Zhang, X. Zhang, Z. Jiang and D. Li, *China Cramics* 1995, 31, 40-44.
8
9 244 4. J. Wu, J. Li, Z. Deng and C. Wang, *Science in China (SERIES E)*, 2004, 34, 516-524.
10
11 245 5. Z. Peng, B. Liang, J. Yu, D. Li, G. Li and J. Zhou, *Science of Conservation and*
12 *archaeology*, 2007, 19, 001-007.
13
14 246
15 247 6. H. S. Cheng, Z. Q. Zhang, H. N. Xia, J. C. Jiang and F. J. Yang, *Nuclear Instruments*
16 *and Methods in Physics Research Section B: Beam Interactions with Materials and Atoms*,
17 248
18 249 2002, 190, 488-491.
19
20 250 7. P. L. Leung and H. Luo, *X-ray Spectrometry*, 2000, 29, 34-38.
21
22 251 8. B.-p. Li, A. Greig, J.-x. Zhao, K. D. Collerson, K.-s. Quan, Y.-h. Meng and Z.-l. Ma,
23 24
25 252 *Journal of Archaeological Science*, 2005, 32, 251-259.
26
27 253 9. B.-P. Li, J.-X. Zhao, A. Greig, K. D. Collerson, Y.-X. Feng, X.-M. Sun, M.-S. Guo and
28 254
29 255 Z.-X. Zhuo, *Journal of Archaeological Science*, 2006, 33, 56-62.
30
31 256 10. A. Mangone, G. E. De Benedetto, D. Fico, L. C. Giannossa, R. Laviano, L. Sabbatini, I.
32 257
33 258 D. van der Werf and A. Traini, *New Journal of Chemistry*, 2011, 35, 2860-2868.
34
35 259 11. J. Pérez-Arantegui, B. Montull, M. Resano and J. M. Ortega, *Journal of the European*
36 260
37 261 *Ceramic Society*, 2009, 29, 2499-2509.
38
39 262 12. M. Resano, J. Perez-Arantegui, E. Garcia-Ruiz and F. Vanhaecke, *Journal of*
40 263
41 264 *Analytical Atomic Spectrometry*, 2005, 20, 508-514.
42
43 265 13. R. Wen, C. S. Wang, Z. W. Mao, Y. Y. Huang and A. M. Pollard, *Archaeometry*, 2007,
44 266
45 267 49, 101-115.
46
47 268 14. D. Zou, Z. Yin, B. Zhang, W. Hang and B. Huang, *Chinese Journal of Analytical*
48 269
49 270 *Chemistry*, 2012, 40, 498-502.
50
51 271 15. L. Burgio, K. Melessanaki, M. Doulgeridis, R. J. H. Clark and D. Anglos,
52 272
53 273 *Spectrochimica Acta Part B: Atomic Spectroscopy*, 2001, 56, 905-913.
54
55 274 16. P. Ballirano and A. Maras, *American Mineralogist*, 2006, 91, 997-1005.
56
57 275 17. H.-L. Yuan, S. Gao, M.-N. Dai, C.-L. Zong, D. Günther, G. H. Fontaine, X.-M. Liu
58 276
59 277 and C. Diwu, *Chemical Geology*, 2008, 247, 100-118.
60 278
279 18. Y. Liu, Z. Hu, S. Gao, D. Günther, J. Xu, C. Gao and H. Chen, *Chemical Geology*,

1
2
3 271 2008, 257, 34-43.
4

5 272 19. Y. Chen, Y. Guo and Z. Zhang, *Journal of the Chinese Ceramic Society*, 1978, 6,
6

7 273 225-241.
8

9 274 20. J. Wu, J. Li and J. Guo, *Journal of Inorganic Material*, 1999, 14, 143-149.
10

11 275
12
13
14
15
16
17
18
19
20
21
22
23
24
25
26
27
28
29
30
31
32
33
34
35
36
37
38
39
40
41
42
43
44
45
46
47
48
49
50
51
52
53
54
55
56
57
58
59
60

1
2
3
4
5
6
7
8
9
10
11
12
13
14
15
16
17
18
19
20
21
22
23
24
25
26
27
28
29
30
31
32
33
34
35
36
37
38
39
40
41
42
43
44
45
46
47
48
49
50
51
52
53
54
55
56
57
58
59
60

276 **Figure captions**

277 Fig.1 three classical blue-and-white porcelains in Ming dynasty from Hongwu (HW),
278 Xuande (XD) and Wangli (WL), which represent three phases: early Ming, middle Ming
279 and late Ming . Each sample can be divided into three areas: dark blue area (-d), light blue
280 area (-l) and white glaze (-w).

281

282 Fig.2 Signal intensity versus time profiles obtained upon ablation of the glazed layer of the
283 XD sample. The cleaning period is not considered for quantification purposes.

284

285 Fig.3 SEM images of cobalt-decorated ceramics. A, image of the thickness of the vitreous
286 layer. B, image of the crater produced by laser ablation

287

288 Fig.4 Triangle diagram relative to iron, manganese and cobalt in light-blue areas and white
289 glaze.

290

291 Fig. 5 Comparison of LA-ICP-MS trace element contents (in $\mu\text{g/g}$) or ratio of dark blue
292 area from Hw, Xd and Wl. Hollow rhombuses are the ratios of HW, while hollow squares
293 are for XD and stuffed triangles are for WL. The error bars are 1σ

294

295 Fig.6 Chondrite-normalized rare-earth-element (REE) patterns showing comparisons
296 among HW, XD and WL. Black real lines are the ratios of HW, while gray lines are for XD
297 and broken lines are for WL.

298

299 Fig.7 the values of Mn, Pb, Ni and Zn correlation coefficient with Co in XD sample.

300

301 Table 1 Instrument operating conditions and data acquisition parameters for the LA-ICP-MS measurements

Geolas laser ablation system					
Laserwave length	193 nm	Energy density	13 J cm ⁻²	Laser Frequency	5 Hz
Number of cleaning pulses	15 pulses	Spot size	60 μm	Number of pulses for analysis	200 pulses
Operating Parameters of ICP-MS					
RF power	1340 W	Carrier gas	1.0 L min ⁻¹	He carrier gas	0.8 L min ⁻¹
Omega lens	12.2 V	Omega bias	-110 V	Extraction 2	-200V
Extraction 1	0 V	Plate bias	-60 V	Deflect	14.2 V
Dwell time per acquisition point	20 ms	Scanning mode	Peak hopping	Sample depth	6.1 mm
Signal monitored	⁷ Li ⁺ , ⁹ Be ⁺ , ¹¹ B ⁺ , ²³ Na ⁺ , ²⁵ Mg ⁺ , ²⁷ Al ⁺ , ²⁹ Si ⁺ , ³¹ P ⁺ , ³⁹ K ⁺ , ⁴³ Ca ⁺ , ⁴⁵ Sc ⁺ , ⁴⁹ Ti ⁺ , ⁵¹ V ⁺ , ⁵³ Cr ⁺ , ⁵⁵ Mn ⁺ , ⁵⁶ Fe ⁺ , ⁵⁹ Co ⁺ , ⁶⁰ Ni ⁺ , ⁶³ Cu ⁺ , ⁶⁶ Zn ⁺ , ⁶⁹ Ga ⁺ , ⁷² Ge ⁺ , ⁷⁵ As ⁺ , ⁸⁵ Rb ⁺ , ⁸⁸ Sr ⁺ , ⁸⁹ Y ⁺ , ⁹⁰ Zr ⁺ , ⁹³ Nb ⁺ , ⁹⁵ Mo ⁺ , ¹¹⁵ In ⁺ , ¹¹⁸ Sn ⁺ , ¹²¹ Sb ⁺ , ¹³³ Cs ⁺ , ¹³⁷ Ba ⁺ , ¹³⁹ La ⁺ , ¹⁴⁰ Ce ⁺ , ¹⁴⁶ Nd ⁺ , ¹⁴⁷ Sm ⁺ , ¹⁵³ Eu ⁺ , ¹⁵⁷ Gd ⁺ , ¹⁵⁹ Tb ⁺ , ¹⁶³ Dy ⁺ , ¹⁶⁵ Ho ⁺ , ¹⁶⁶ Er ⁺ , ¹⁶⁹ Tm ⁺ , ¹⁷² Yb ⁺ , ¹⁷⁵ Lu ⁺ , ¹⁷⁸ Hf ⁺ , ¹⁸¹ Ta ⁺ , ¹⁸² W ⁺ , ²⁰⁵ Tl ⁺ , ²⁰⁸ Pb ⁺ , ²⁰⁹ Bi ⁺ , ²³² Th ⁺ , ²³⁸ U ⁺ .				

302

303

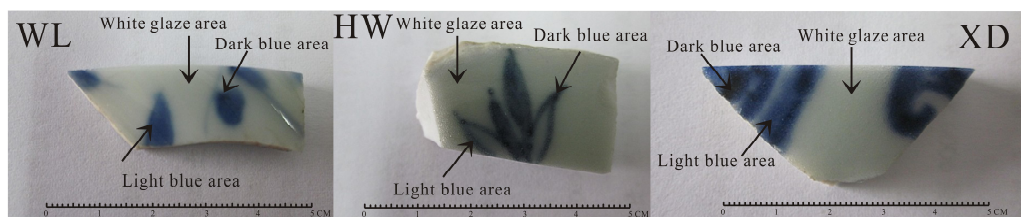
1
2
3
4
5
6
7
8
9
10
11
12
13
14
15
16
17
18
19
20
21
22
23
24
25
26
27
28
29
30
31
32
33
34
35
36
37
38
39
40
41
42
43
44
45
46
47
48
49
50
51
52
53
54
55
56
57
58
59
60

304 Table 2 The Mn, Fe and Co concentrations of white, light-blue and dark-blue areas of the three selected
 305 samples of HW, XD and WL.

		Mn	Fe	Co	Fe/Mn
HW-white		591	6940	1.08	11.8
		593	6564	1.10	11.1
		590	6502	1.14	11.0
		608	7251	1.28	11.9
		576	6535	1.42	11.3
		648	7508	1.84	11.6
	Average±1s	601±25.2	6883±424	1.31±0.29	11.5±0.37
RSD	4.19	6.15	22.1	3.26	
HW-light		496	5675	41.5	11.4
		565	6720	81.5	11.9
		533	6692	105	12.5
		540	6477	111	12.0
		575	6823	112	11.9
	Average±1s	542±30.9	6477±466	90.2±29.9	11.9±0.39
	RSD	5.70	7.19	33.1	3.28
HW-dark		526	6369	130	12.1
		491	5886	135	12.0
		652	7440	164	11.4
		670	9143	418	13.6
		751	19867	1796	26.4
	Average±1s	618±107	9741±5707	529±719	618±107
	RSD	17.4	59.5	136	42.2
XD-white		562	6296	7.79	11.2
		427	4922	8.60	11.5
		633	6689	12.1	10.6
		541	6084	13.4	11.3
		633	6442	13.8	10.2
		537	5425	15.2	10.1
	Average±1s	551±70.9	5900±645	12.8±3.85	10.8±0.57
RSD	12.9	10.9	30.0	5.3	
XD-light		2762	6401	413	2.32
		2551	7589	420	2.97
		2330	6569	459	2.82
		3340	5680	549	1.70
		3789	8957	636	2.36
		4652	7905	732	1.70
	Average±1s	3237±876	7184±1190	535±129	2.31±0.54
RSD	27.1	16.6	24.1	23.2	
XD-dark		11545	11426	2124	0.99
		14158	13076	2870	0.92
		15559	15734	2892	1.01
		17240	15616	3079	0.91
		17276	15361	3183	0.89
		22299	14529	4696	0.65
	Average±1s	17660±4797	14593±1759	3487±1199	0.86±0.15
RSD	27.2	12.1	34.4	17.7	
WL-white		676	9776	19.1	14.5
		667	10080	29.2	15.1
		681	10081	33.3	14.8
		673	9924	37.1	14.7
		675	10298	47.2	15.3
		704	10596	67.4	15.0
	Average±1s	679±12.9	10126±289	38.9±16.7	14.9±0.29
RSD	1.90	2.86	43.1	1.95	
WL-light		2593	12330	2105	4.76
		1317	12900	2412	9.80
		1956	13252	2844	6.77
		1963	13781	3822	7.02
	Average±1s	1957±521	13066±610	2796±748	7.09±2.07
	RSD	26.6	4.67	26.8	29.2
	WL-dark		4019	13191	2709
		2195	13870	3967	6.32
		5284	15625	5248	2.96
		1783	13716	3918	7.69
		1565	12730	3597	8.13
Average±1s		2969±1615	13826±1102	3888±913	5.68±2.43
RSD		54.4	7.97	23.5	42.8

306

307



308

309

Fig.1 three classical blue-and-white porcelains in Ming dynasty from Hongwu (HW),

310

Xuande (XD) and Wangli (WL), which represent three phases: early Ming, middle Ming

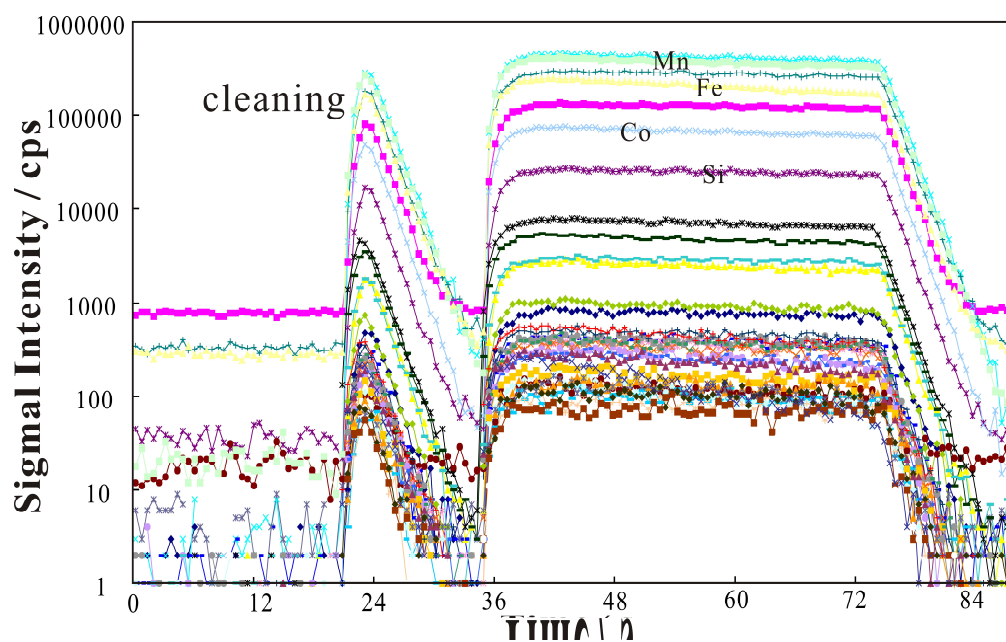
311

and late Ming . Each sample can be divided into three areas: dark blue area (-d), light blue

312

area (-l) and white glaze (-w).

313

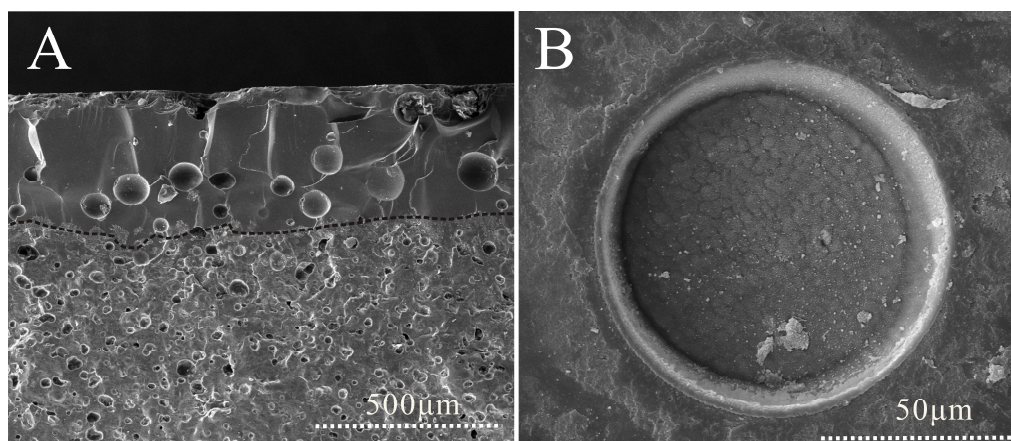


314

315 Fig.2 Signal intensity versus time profiles obtained upon ablation of the glazed layer of the

316 XD sample. The cleaning period is not considered for quantification purposes.

317



318

319 Fig.3 SEM images of cobalt-decorated ceramics. A, image of the thickness of the vitreous

320 layer. B, image of the crater produced by laser ablation

321

1
2
3
4
5
6
7
8
9
10
11
12
13
14
15
16
17
18
19
20
21
22
23
24
25
26
27
28
29
30
31
32
33
34
35
36
37
38
39
40
41
42
43
44
45
46
47
48
49
50
51
52
53
54
55
56
57
58
59
60

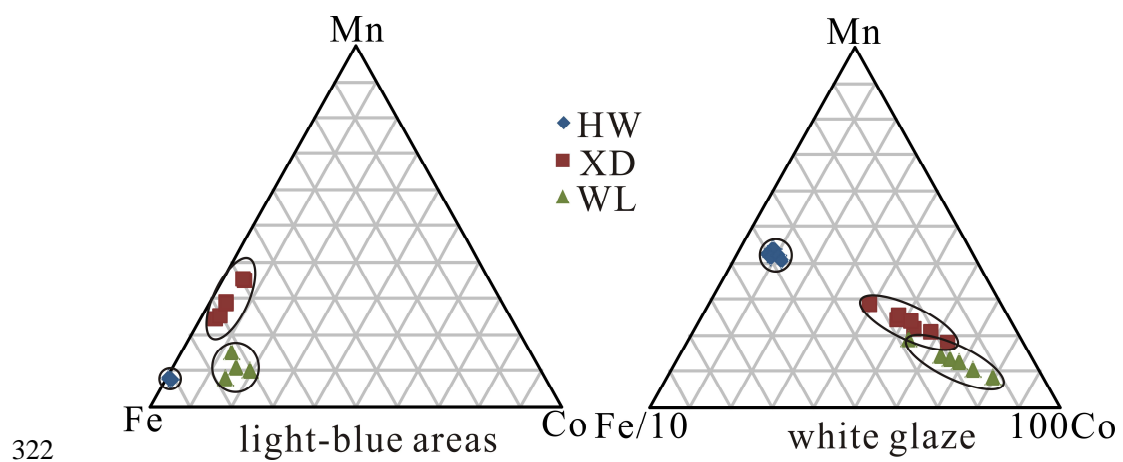
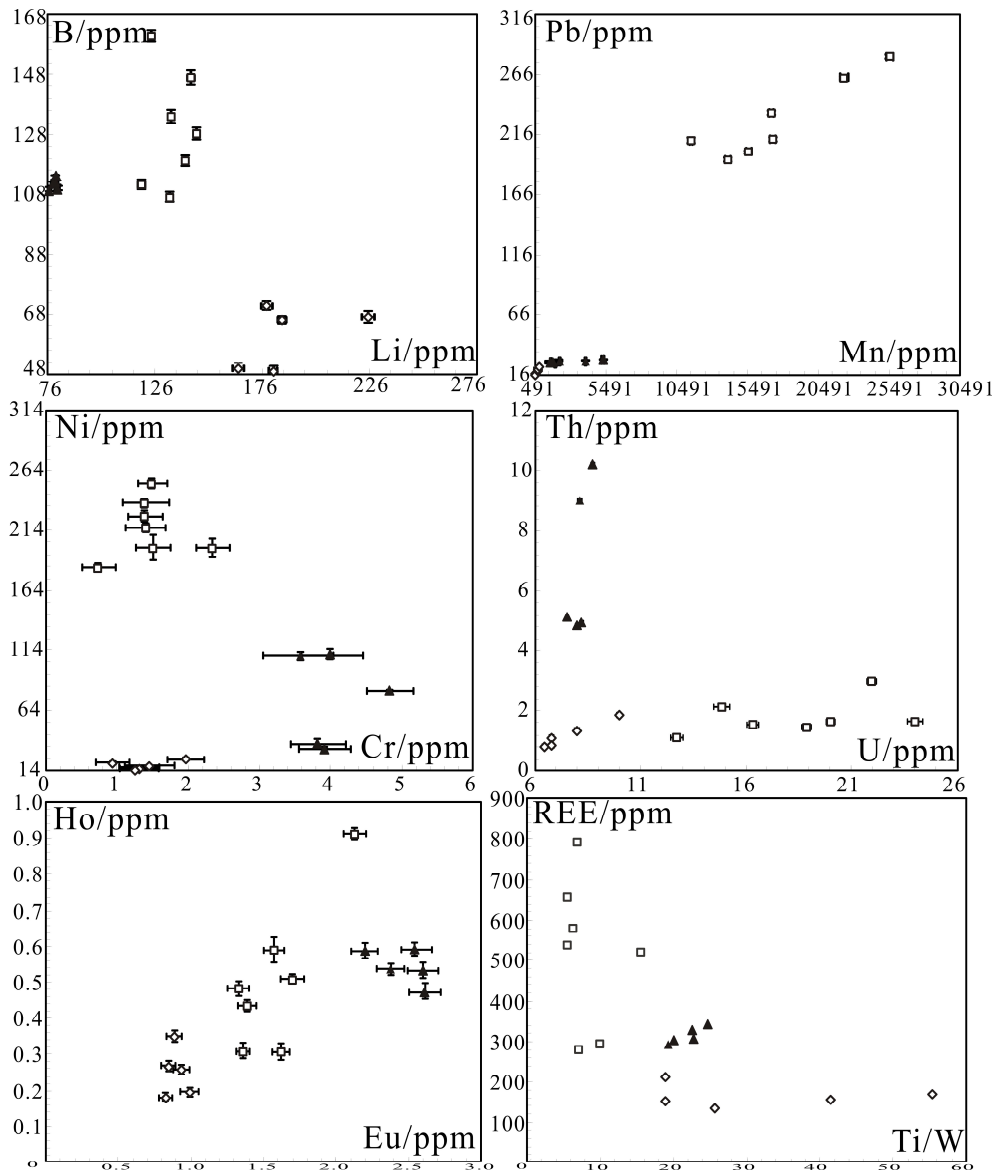


Fig.4 Triangle diagram relative to iron, manganese and cobalt in light-blue areas and white glaze.



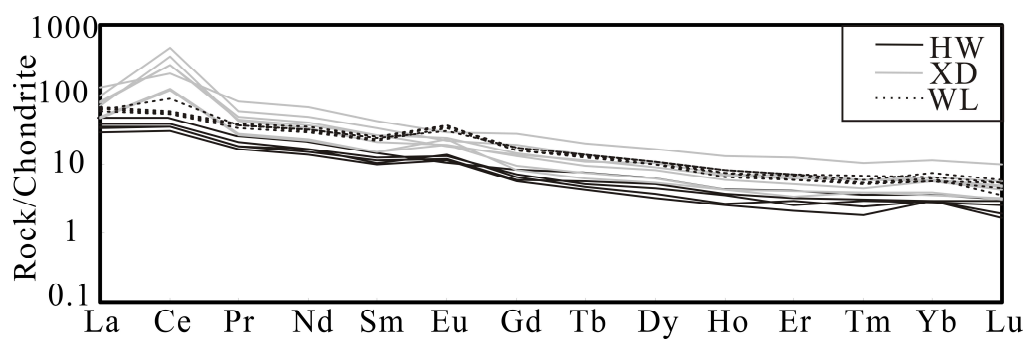
326

327 Fig. 5 Comparison of LA-ICP-MS trace element contents (in $\mu\text{g/g}$) or ratio of dark blue

328 area from Hw, Xd and Wl. Hollow rhombuses are the ratios of HW, while hollow squares

329 are for XD and stuffed triangles are for WL. The error bars are 1σ

330



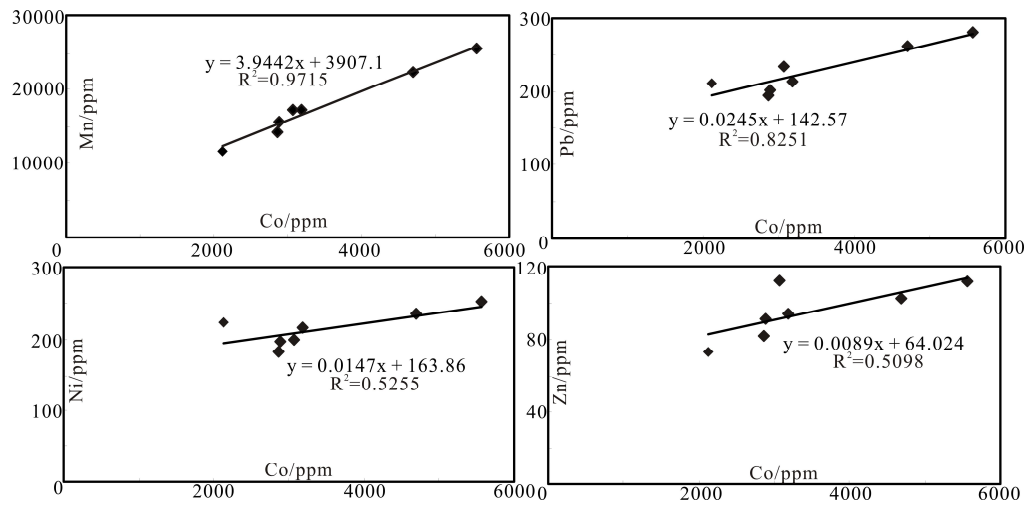
331

332 Fig.6 Chondrite-normalized rare-earth-element (REE) patterns showing comparisons

333 among HW, XD and WL. Black real lines are the ratios of HW, while gray lines are for XD

334 and broken lines are for WL.

335



336

337 Fig.7 the values of Mn, Pb, Ni and Zn correlation coefficient with Co in XD sample.

338